Testing the state of bedform equilibrium using MBES data form the Mekong River, Cambodia

Christopher A. Unsworth *University of Hull, Hull, UK – christopher.unsworth@hull.ac.uk*
Daniel R. Parsons *University of Hull, Hull, UK – d.parsons@hull.ac.uk*
Christopher Hackney *University of Hull, Hull, UK – c.hackney@hull.ac.uk*
James Best: *Departments of Geography and Geographic Information Science, Mechanical Science and Engineering and Ven Te Chow Hydrosystems Laboratory, University of Illinois, 1301 W. Green St., Urbana, IL 61801, USA - jimbest@illinois.edu*
Stephen E. Darby *Geography and Environment, University of Southampton, Southampton SO17 1BJ, UK - S.E.Darby@soton.ac.uk*
Julian Leyland *Geography and Environment, University of Southampton, Southampton SO17 1BJ, UK - J.Leyland@soton.ac.uk*
Andrew P. Nicholas *Department of Geography, University of Exeter, Exeter EX4 4RJ, UK - A.P.Nicholas@exeter.ac.uk*
Rolf Aalto *Department of Geography, University of Exeter, Exeter EX4 4RJ, UK- Rolf.Aalto@exeter.ac.uk*

ABSTRACT: In this short paper, we demonstrate a new method of deciphering the state of non-equilibrium bedforms using Semi-Variograms. Semi-variograms allow us to take a measure of uniformity in repeating features; therefore, the technique implicitly assumes that equilibrium is defined by uniformity. Comparison of the semi variogram produced from 5 selected profiles of dunes at different states of equilibrium and boundary conditions from the Mekong River (Cambodia) is compared against the semi variogram produced from an idealised and identical train of bedforms. We find that the empirical semi-variogram of a bedform profile is more than adequate at estimate the mean length of the bedforms, can decipher the dominant scales of bedforms. Moreover, this technique opens up the possibility of quantifying the degree of dis-equilibrium in the bed state that departs from basic geometric measurement of height, length and aspect ratio, and also does not require a series of repeated measurements: which is uncommon in large MBES surveys.

1 INTRODUCTION

Equilibrium in bedform state is described as a series of repeating bed features with consistent height, length and shape in time and space, and whilst many definitions attempt to describe predict the geometric size of the bedform in relation to grain size, flow depth or bed shear stress (Baas, 1994, 1999; Bartholdy et al., 2002; Dreano et al., 2010; Flemming, 2000; Martin & Jerolmack, 2013; Myrow et al., 2018; Perillo et al., 2014; Reesink et al., 2018), here we are only investigating the consistency in bedform shape in space. Such a definition of equilibrium requires a geometric uniformity perhaps unlikely with some definitions of equilibrium and three-dimensional bedforms (Myrow et al., 2018; Reesink et al., 2018) but no less can define the end member to the broad spectrum of bedform disequilibrium. A fundamental properly of uniquely repeating shapes is that they are "self-similar" at their own spatial and temporal scales, implying a measure of equilibrium (or disequilibrium) is plausible from their correlation. For features which display spatial linkages, the semi-variogram is preferred over auto-correlation due to the semi-variograms' inherent spatial-dependency (Clifford et al., 1992; Matheron, 1965; Oliver & Webster, 1986; Qin et al., 2015). A train of dunes, for instance, displays a range of spatial linkages:

1) alteration of the downstream pressure gradient and the production and dissipation rates of turbulence over bedforms (Engel,

1981; Kadota & Nezu, 1999; Unsworth et al., 2018).

2) changing the rate of sediment supply though altering the ratio of suspended to bedload fraction (Naqshband et al., 2014; Reesink et al., 2018; Schindler & Robert, 2005; Wren et al., 2007), largely a response to bedform interactions in or out of equilibrium (Blois et al., 2012; Ewing & Kocurek, 2010; Reesink et al., 2018).

The semi-variance $\gamma(h)$ of a random function $(G(X))$ is described by half the variance of the increment:

$$2\gamma(h) = Var[G(x+h) - G(x)] \quad (1)$$

Where G is the random variable of interest, h is the lag or distance with respect to x. The empirical semi variance is estimated by:

$$2\gamma(h) = \left[\frac{1}{N-h}\right] \sum_{i=1}^{N-h} [(x_i + h) - G(x_i)]^2 \quad (2)$$

Where N is the number of observations.

The semi-variogram of three types of dune shapes is described in Figure 1. In this figure the maximum lag distance h_{max} has been set to the same length scale as the length of the bedform profiles so any variation in the shape of the dunes would be picked up.

The shape of the variogram appears to not correspond to the shape or asymmetry of the bedform – it is always a sine wave when given identical repeating bedform. This is a useful feature as we wish to test this method of quantifying equilibrium on a range of bedform shapes.

To provide a range of realistic bed states to test these ideas on, Multibeam echosounder (MBES) bathymetry from the Mekong River in Cambodia is used as it provides a range of flow discharges, bedform states and is large enough that superimposed bedforms are well resolved in the bathymetry.

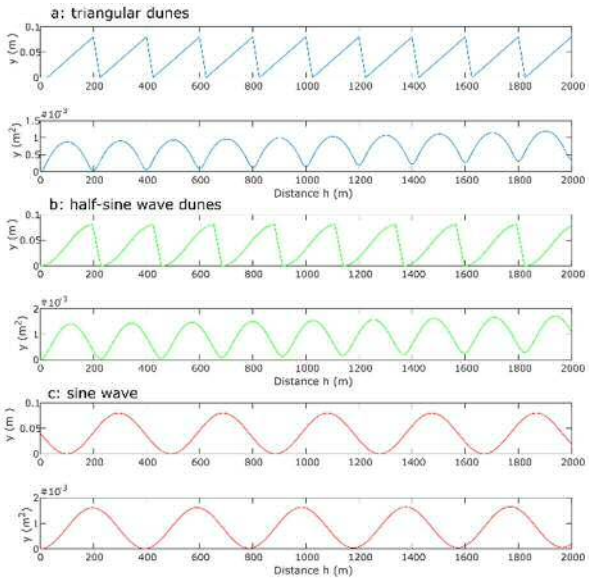

Figure 1. Three sets of idealised repeating dune shapes and their semi-variogram. The triangular dunes in a) are those form (Unsworth et al., 2018); b) half-sine wave shape is from (Nelson et al., 1993). The repeating dune shapes produce a sine-wave in the semi-variogram that is correlated to the dune troughs – where the profiles begin. The location of each trough in the semi-variograms directly corresponds to the wavelength of the bedform. The sine wave bedforms in c) provide a symmetrical bedform profile, the semi-variogram of which produces a sine wave 45 degrees out of phase.

1 2 METHODS

2.1 Study Area

The Mekong is one of the world's largest rivers, with a mean annual discharge of 457 km^3 draining an area of 795,000 km^2 and a mean annual sediment load of 1.68 t (MRC 2010; Gupta & Liew 2007; Milliman & Meade 1983). Annual rainfall is high over the northern and eastern basin (2000–4000+ mm yr^{-1}), decreasing over the lowland areas, (~1000mm a year) (Gupta & Liew, 2007). However this rainfall is highly seasonal with 85-90% falling between June and October in the South-western monsoon season. This produces large flood events on the order of 30,000 to 60,000 m^3s^{-1} that provide 80% of the mean annual discharge for the river (MRC 2005). The Mekong River basin north of the town of Kratie, Cambodia, is largely bedrock controlled. The Mekong travels 4000km from its source (out of a total length of 4880km) before reaching the Cambodian

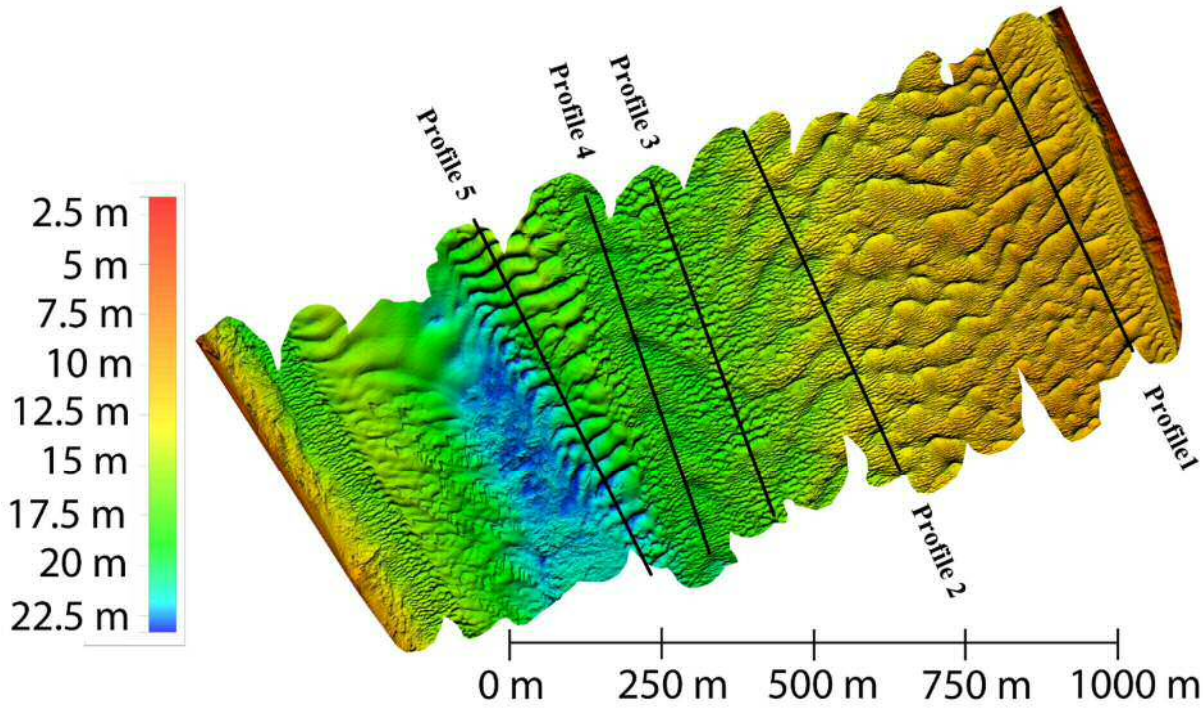

Figure 2 MBES bathymetry of the Mekong River, near Kratie 24/09/2013 at a flood peak discharge of ~60,000 m^3s^{-1}. Gridded resolution is 0.5 m.

alluvial plain near Kratie (Gupta & Liew 2007). By this point, 95% of the total Mekong flow has entered the river (MRC 2005) and the mostly bedrock nature of the upper reaches means the Mekong at Kratie receives the peak flood flows with little upstream attenuation. The inter-annual river discharge changes dramatically between monsoon and dry seasons, with changes in stage of 20-30m being common and corresponding discharge changes from <5,000 m^3s^{-1} in the dry season to an average of 35,000 m^3s^{-1} in the wet which peaks at ~60,000 m^3s^{-1}.

2.2 Data Collection Instruments, accuracy and correction.

An MBES field survey was undertaken on the Mekong river, Cambodia ~12km south of
the transition from bedrock channel to gravel and sand. The complex river bed bathymetry was measured with a Reson© SeaBat© SV2 7125 Multibeam (MBES) at a gridded horizontal resolution of 0.5m on 24/09/2013. The MBES positioning was measured using a real-time kinematic GPS accurate to 0.02 m horizontally and 0.03 m vertically. The manufacturer reported that depth resolution of the MBES is 1.25 cm [Reson Inc., 2009]. The head generates 512 equidistant beams and measures relative water depths over a 150° wide swath perpendicular to the vessel track. Navigation, orientation, and attitude data (heave, pitch, and roll) were recorded using an Applanix POS MV V3 gyroscope inertial guidance system mounted inside the vessel. The MBES data was measured and corrected concurrently using this dGPS and gyroscope setup, with additional acoustic correction using a RESON SVP sound velocity profiler.

3 RESULTS:

Figure 3 displays the bed profile and empirical semi-variogram of bed Profile 1 (see Figure 1 for location). In this section of the DEM, group average dune height = 0.84 m; Length = 38 m; Stoss slope = 3.2°; Lee slope = 19°) with mildly sinuous crest lines. This section of the river is often exposed or <1m deep in the dry season. At the time of measurement, flow stage was at its 3rd high-

est on record and all the river bed was fully submerged. This section of dunes has superimposed bedforms with group average dimensions of ~0.17 m height, 5.17 m length, stoss side angle of 7° and lee side angle of 14°. The empirical semi-variogram in Figure 3F displays zero nugget, a gaussian curve with a range of 37m– very closely matching the hand measured mean wavelength. At longer lag distances than the range, a distorted sine wave is produced, indicating divergence from ideal equilibrium.

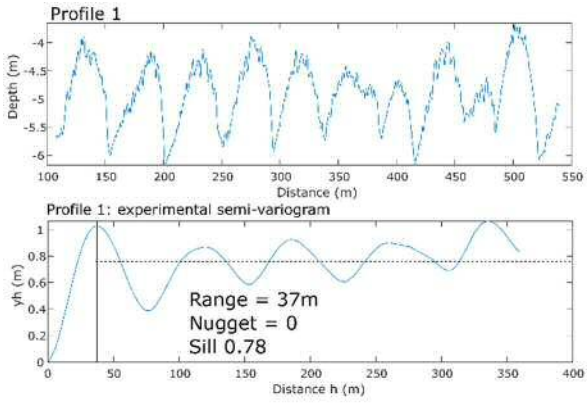

Figure 3. Displays the de-trended bed profile 1 (top) and its empirical semi-variogram (bottom).

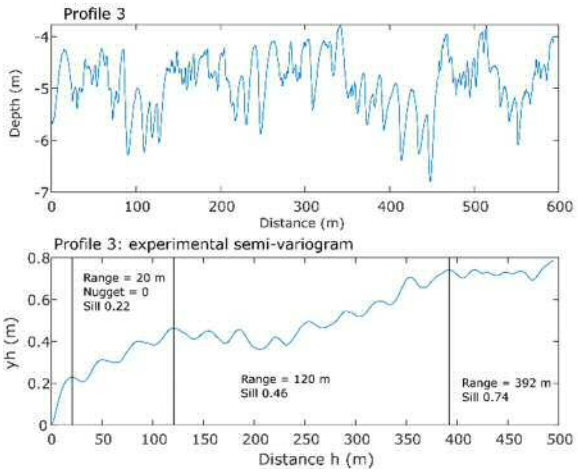

Figure 4. Displays the de-trended bed profile 3 (top) and its empirical semi-variogram (bottom).

Figure 4 displays multiple scales of bedforms superimposed on a varying mean depth. The empirical semi-variogram for this profile likewise produces several scales: 20 m, 120m and 394 m as defined by the range, and two fluctuating sills. Hand measured group mean dune heights are 0.89 m, length 18.6m stoss slope = 9.68°, lee slope 21.9°.

Figure 5 displays the bed profile and semi-variogram across a section of barchanoid shaped dunes with considerable bedform superposition on both stoss and lee slopes. Here the semi-variogram produced two distinct sills with elevations dissimilar to those of the host (length 78m, height 1.5m) and superimposed dunes (4.9 m long and 0.27 m high). The two distinct scales of undulating topography indicate a distinct lack of equilibrium in bedform shape but also indicate that the semi-variogram is less capable of measuring bedform scale which such a range of bedform scales.

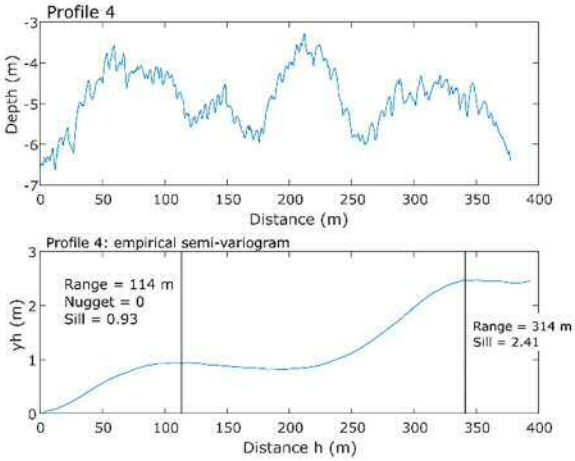

Figure 5. Displays the de-trended bed profile 4 (top) and its empirical semi-variogram (bottom).

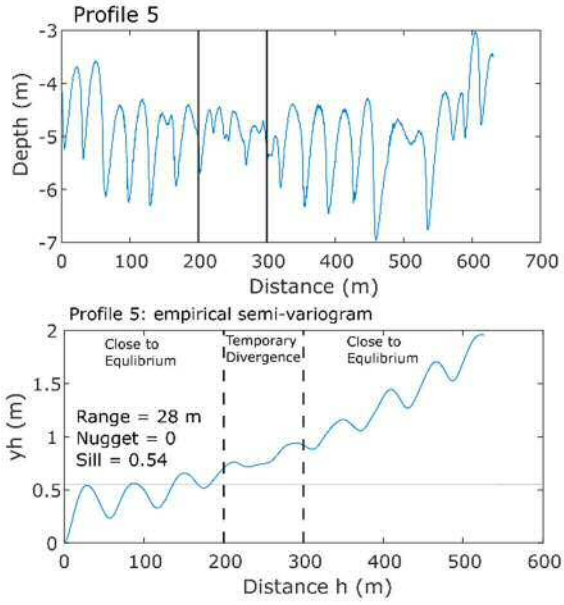

Figure 6. Displays the de-trended bed profile 5 (top) and its empirical semi-variogram (bottom).

Figure 6 displays the bed profile of a section of bed where bedforms are migrating off the tail of a mid-channel bar. There is a complete lack of superimposed bedforms in the section. The lateral extent of the uniform 2D dunes is ~170m wide at the northern extent and is gradually reduced to 70m in width at the southern extent of the survey area, as the 2D dunes merge with the secondary dunes near bed profile 4. A profile taken through the centre of this train of dunes using the MBES data gives a very consistent dune geometry (Figure 6), with group mean heights of ~ 1.6m, lengths of 34m, Stoss slope angle of 6.8° and Lee slopes of 22°. The consistency of dune shape and size is surprising considering the change in depth across the transect of 15 to 22m. Despite this change in boundary condition, the dune 2D and planform shape and size is remarkably regular and the empirical semi-variogram attests to this regularity, producing regular sine waves until ~200-300m where a sequence of smaller dunes produces a temporary sill in the semi-variogram.

To compare the empirical semi-variograms produced from the bedform profiles in Figures 3-6, Figure 7 plots them all normalised by the range of each semi-variogram alongside the idealised triangular dune profile semi-variogram of Figure 1.

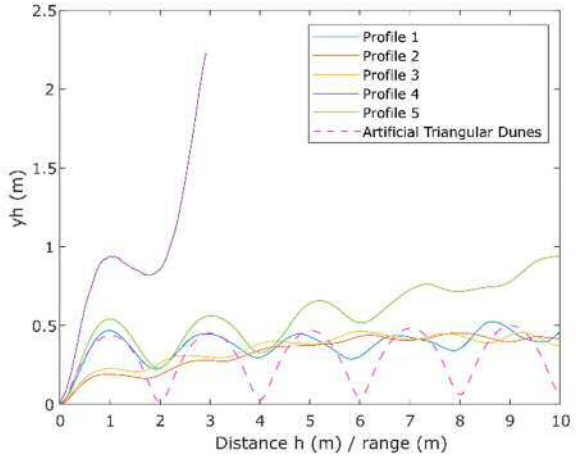

Figure 7. Empirical semi-variograms for all bedform profiles, as well as the idealised triangular dunes in Figure 1. The lag distance h has been normalised by the respective ranges.

Figure 7 Produces the observation that if you normalise the semi variogram by the range of the semi-variogram; the close-to equilibrium bedform profiles overlap. Here we see that the semi-variograms of profiles 1 and 5 most closely those of the idealised dune forms – with peaks and troughs of matching from 3-4 wavelengths. The semi-variograms of Profiles 2 and 3 are more like each other than the idealised bedform profile – suggesting a lateral connectivity to the amount of dis-equilibrium of the bed state measured in Profiles 2 and 3. Profile 4 displays the furthest match with the idealised dune semi-variogram. As seen in Figure 2 and 5, this bedform profile consists of two distinct scales of bedforms, larger barchan shapes but also smaller bedforms migrating over the barchan bedforms on both lee and stoss slopes as also seen in the Amazon (Almeida et al., 2016). The train of barchan dunes is present in this location during the dry season and with a difference in discharge of ~ 45,000 m^3s^{-1} between low and high flows in 2013 it is certainly not unreasonable that these barchan-like bedforms are being eroded at this stage.

5 CONCLUSIONS

By comparing the empirical semi-variogram produced from an idealised train of dunes with the empirical semi-variogram produced from a range of real bedform profiles we found that it is, at present, qualitatively possible to define the degree of (dis) equilibrium of a single bedform profile. This technique and observation opens up a new way of quantifying the state of equilibria in a train of bedforms that does not require a repeated set of measurements over time – as is uncommon in large scale MBES surveys.

6 ACKNOWLEDGEMENTS

This study was supported by awards NE/JO21970/1, NE/JO21571/1 and NE/JO21881/1 from the UK Natural Environmental Research Council (NERC) and

the Academy of Finland funded project SCART (grant number 267463).

7 REFERENCES

Almeida, R. P. de, Galeazzi, C. P., Freitas, B. T., Janikian, L., Ianniruberto, M., & Marconato, A. 2016. Large barchanoid dunes in the Amazon River and the rock record: Implications for interpreting large river systems. Earth and Planetary Science Letters, 454, 92–102.

Baas, J. H. 1994. A Flume Study on the Development and Equilibrium Morphology of Current Ripples in Very Fine Sand. Sedimentology, 41(2), 185–209.

Baas, J. H. 1999. An empirical model for the development and equilibrium morphology of current ripples in fine sand. Sedimentology, 46, 123–138.

Bartholdy, J., Bartholomae, A., & Flemming, B. 2002. Grain-size control of large compound flow-transverse bedforms in a tidal inlet of the Danish Wadden Sea. Marine Geology, 188, 391–413.

Blois, G., Barros, J. M., Christensen, K. T., & Best, J. L. 2012. An experimental investigation of 3D subaqueous barchan dunes and their morphodynamic processes. In Marine and River Dune Dynamics 4 (pp. 35–38).

Clifford, N. J., Robert, A., & Richards, K. S. 1992. Estimation of flow resistance in gravel-bedded rivers: A physical explanation of the multiplier of roughness length. Earth Surface Processes and Landforms, 17(2), 111–126.

Dreano, J., Valance, A., Lague, D., & Cassar, C. 2010. Experimental study on transient and steady-state dynamics of bedforms in supply limited configuration. Earth Surface Processes and Landforms, 35(14), 1730–1743.

Engel, P. 1981. Length of flow seperation over dunes. Journal of Hydraulic Division. American Society of Civil Engineers, 107(HY10), 113–1143.

Ewing, R. C., & Kocurek, G. A. 2010. Aeolian dune interactions and dune-field pattern formation: White Sands Dune Field, New Mexico. Sedimentology, 57, 1199–1219.

Flemming, B. W. 2000. The role of grain size, water depth and flow velocity as scaling factors controlling the size of subaqueous dunes. In I. A. T. &T. G. (eds). (Ed.), Proceedings of Marine Sandwave Dynamics (pp. 55–61). Lille, France.

Kadota, A., & Nezu, I. 1999. Three-dimensional structure of space-time correlation on coherent vortices generated behind dune crest. Journal of Hydraulic Research, 37(1), 59–80.

Martin, R. L., & Jerolmack, D. J.(2013. Origin of hysteresis in bed form response to unsteady flows. Water Resources Research, 49(3), 1314–1333.

Matheron, G. 1965. Les Variables Regionalisees et Leur Estimation. Paris: Masson.

Myrow, P. M., Jerolmack, D. J., & Perron, J. T. 2018. Bedform Disequilibrium. Journal of Sedimentary Research, 88(9), 1096–1113.

Naqshband, S., Ribberink, J. S., Hurther, D., & Hulscher, S. J. M. H. 2014. Bed load and suspended load contributions to migrating sand dunes in equilibrium. Journal of Geophysical Research: Earth Surface, 119(5), 1043–1063.

Nelson, J. M., McLean, S. R., & Wolfe, S. R. 1993. Mean Flow and Turbulence Fields Over Two-Dimensional Bed Forms. Water Resources Research, 29(12), 3935–3953.

Oliver, M. A., & Webster, R. 1986. Semi-Variogram for modelling the sptail pattern of landform and soail properties. Earth Surface Processes and Landforms, (11), 491–501.

Perillo, M. M., Best, J. L., Yokokawa, M., & Sekiguchi, T. 2014. A unified model for bedform development and equilibrium under unidirectional, oscillatory and combined-flows. Sedimentology,7 (61), 2063-2085

Qin, J., Wu, T., & Zhong, D. 2015. Spectral behavior of gravel dunes. Geomorphology, 231, 331–342.

Reesink, A. J. H., Parsons, D. R., Ashworth, P. J., Best, J. L., Hardy, R. J., Murphy, B. J., et al. 2018. The adaptation of dunes to changes in river flow. Earth-Science Reviews, 185, 1065–1087

Schindler, R. J., & Robert, A. 2005. Flow and turbulence structure across the ripple-dune transition: an experiment under mobile bed conditions. Sedimentology, 52(3), 627–649.

Unsworth, C. A., Parsons, D. R., Hardy, R. J., Reesink, A. J. H., Best, J. L., Ashworth, P. J., & Keevil, G. M. 2018. The Impact of Nonequilibrium Flow on the Structure of Turbulence Over River Dunes. Water Resources Research, 54(9), 6566–6584.

Wren, D. G., Kuhnle, R. A., & Wilson, C. G. 2007. Measurements of the relationship between turbulence and sediment in suspension over mobile sand dunes in a laboratory flume. Journal of Geophysical Research, 112(F3).